Acta Pharmacologica Sinica

www.nature.com/aps

ARTICLE

OTUD1 promotes hypertensive kidney fibrosis and injury by deubiquitinating CDK9 in renal epithelial cells

Meng-yang Wang[1,2,3], Tian-xiang Yu[1,2], Qin-yan Wang[1,2], Xue Han[1,2], Xiang Hu[4], Shi-ju Ye[2], Xiao-hong Long[2], Yi Wang[2], Hong Zhu[4], Wu Luo[2]✉ and Guang Liang[1,2,5]✉

Hypertensive renal disease (HRD) contributes to the progression of kidney dysfunction and ultimately leads to end-stage renal disease. Understanding the mechanisms underlying HRD is critical for the development of therapeutic strategies. Deubiquitinating enzymes (DUBs) have been recently highlighted in renal pathophysiology. In this study, we investigated the role of a DUB, OTU Domain-Containing Protein 1 (OTUD1), in HRD models. HRD was induced in wild-type or *Otud1* knockout mice by chronic infusion of angiotensin II (Ang II, 1 μg/kg per min) through a micro-osmotic pump for 4 weeks. We found that OTUD1 expression levels were significantly elevated in the kidney tissues of Ang II-treated mice. *Otud1* knockout significantly ameliorated Ang II-induced HRD, whereas OTUD1 overexpression exacerbated Ang II-induced kidney damage and fibrosis. Similar results were observed in TCMK-1 cells but not in SV40 MES-13 cells following Ang II (1 μM) treatment. In Ang II-challenged TCMK-1 cells, we demonstrated that OTUD1 bound to CDK9 and induced CDK9 deubiquitination: OTUD1 catalyzed K63 deubiquitination on CDK9 with its Cys320 playing a critical role, promoting CDK9 phosphorylation and activation to induce inflammatory responses and fibrosis in kidney epithelial cells. Administration of a CDK9 inhibitor NVP-2 significantly ameliorated Ang II-induced HRD in mice. This study demonstrates that OTUD1 mediates HRD by targeting CDK9 in kidney epithelial cells, suggesting OTUD1 is a potential target in treating this disease.

Keywords: hypertensive renal disease; OTUD1; Ang II; deubiquitination enzyme; CDK9

Acta Pharmacologica Sinica (2024) 45:765–776; https://doi.org/10.1038/s41401-023-01192-6

INTRODUCTION

The prevalence of hypertension, a principal factor responsible for kidney damage, is escalating worldwide [1]. Chronic hypertension often culminates in a condition known as hypertensive nephropathy or hypertensive renal disease (HRD). Hypertension-associated organ damage primarily stems from the exaggerated cellular response and vascular structure alterations, characterized by cytokine secretion from immune cells, matrix degradation, and fibrosis [2]. Key factors instigating and furthering HRD include renal inflammation and fibrosis [3]. Substantial evidence indicates that renal damage activates the intrarenal renin-angiotensin system (RAS) by upregulating several RAS component genes, such as renin, Ang type 1 receptor [4], angiotensin-converting enzyme (ACE), and angiotensinogen. The two salient enzymes in the RAS, ACE and renin, synthesize the primary active peptide, Angiotensin II (Ang II). This peptide incites renal injury, irrespective of its dependence on blood pressure. Therefore, understanding hypertensive nephropathy's pathogenesis and identifying potential therapeutic targets are of paramount scientific and clinical importance in preventing and treating HRD.

Chronic pathological conditions often involve changes in regulatory or causative cellular protein levels. The lysosomal and ubiquitin-proteasome systems in eukaryotic cells primarily regulate protein turnover [5, 6]. The ubiquitin-proteasome system includes the deubiquitinases (DUBs), the ubiquitination machinery, ubiquitin (UB), and proteasome, influencing various cellular processes, including cell signaling, cell fate determination, and inflammatory responses [7, 8]. Recently, DUBs have been considered to play significant roles in nephropathy. A study has demonstrated that the USP11, a deubiquitinating enzyme, instigates renal tubular cell senescence and fibrosis by inhibiting the TGF-β receptor II ubiquitin degradation [3]. However, it is unclear whether DUBs regulate the pathogenesis of HRD. OTUD1 is a DUB, which is encoded on chromosome 10p12.2 as a single exon with a molecular mass of 51 kDa comprising 481 residues [9]. OTUD1 has been linked with cancer, immune response, and inflammation. For instance, OTUD1 has demonstrated the ability to bolster iron transport and augment antitumor immunity in colon cancer by modulating the iron-responsive element-binding protein 2 [10]. An engaging goal of our lab is to demonstrate the role and mechanisms of ubiquitin homeostasis in hypertensive complications and find new therapeutic strategies for these diseases. Studying OTUD1 in HRD here originates from an accidental finding in our previous study, where we have

[1]Department of Pharmacy and Institute of Inflammation, Zhejiang Provincial People's Hospital, Affiliated People's Hospital, Hangzhou Medical College, Hangzhou 310014, China; [2]Chemical Biology Research Center, School of Pharmaceutical Sciences, Wenzhou Medical University, Wenzhou 325035, China; [3]Department of Pharmacology, College of Pharmacy, Beihua University, Jilin 132013, China; [4]Department of Endocrinology, the First Affiliated Hospital of Wenzhou Medical University, Wenzhou 325035, China and [5]School of Pharmaceutical Sciences, Hangzhou Medical College, Hangzhou 310014, China
Correspondence: Wu Luo (wuluo@wmu.edu.cn) or Guang Liang (wzmcliangguang@163.com)
These authors contributed equally: Meng-yang Wang, Tian-xiang Yu

Received: 17 June 2023 Accepted: 5 November 2023
Published online: 18 December 2023

demonstrated that cardiomyocyte OTUD1 mediates Ang II-induced cardiac hypertrophy by deubiquitinating STAT3 [11]. We have also found that OTUD1 in mouse endothelial cells is known to foster Ang II-induced vascular remodeling *via* SMAD3 deubiquitination [12]. Nonetheless, OTUD1's role in HRD remains unexplored.

Therefore, we tried to examine the gene expression profile of OTUD1 in the kidney tissues of Ang II-infused mice, and interestingly, we identified the increased level of renal OTUD1 interestingly, indicating an involvement of OTUD1 in HRD. This study examines the role of OTUD1 in hypertensive nephropathy. We revealed that OTUD1 interacts with cyclin-dependent kinase 9 (CDK9) to induce CDK9 deubiquitination and increase its phosphorylation. This, in turn, the expression of genes associated with renal inflammation and fibrosis was amplified. These findings uncover OTUD1 as a key regulator in HRD and identity CDK9 as a substrate protein of OTUD1.

MATERIALS AND METHODS

Reagents

Angiotensin II (cat# 4474913) was procured from Aladdin (Shanghai, China), while OTUD1 scrambled sequences and siRNA were obtained from GenePharma (Shanghai, China). Plasmids HA-CDK9, Flag-OTUD1, Myc-UB, Myc-K63, Myc-K48, as well as an empty vector and AAV9 for OTUD1 expression, were sourced from Genechem (Shanghai, China). The OTUD1 antibody (orb185712) was purchased from Biorbyt (Cambridge, UK), and antibodies against TGF-β1 (ab179695), collagen IV (COL-IV; ab6586), Aquaporin 1 (AQP-1; ab168387), and desmin (ab32363) were procured from Abcam (Cambridge, UK). CDK9 (2316), phospho (Thr186)-CDK9 (2549), NF-κB p65 (8242), phosphorylated p65 (p-p65, 3033), and GAPDH (5174) antibodies were bought from Cell Signaling Technology (Danvers, MA, USA). Rabbit IgG (B900610) and antibodies against Flag (20543-1-AP), Myc (16286-1-AP), and HA (51064-2-AP) were sourced from Proteintech (Rosemont, IL, USA). ELISA kit for Ang II was obtained from Shanghai Tongwei Biological Technology Co., Ltd (Shanghai, China). Creatinine (Cr; cat# C011-2-1), urinary albumin (Alb; cat# E038-1-1) and blood urea nitrogen (BUN; cat# C013-2-1) kits were obtained from Nanjing Jiancheng Bioengineering Institute (Nanjing, China). Masson's Trichrome kit (cat# G1340), Picrosirius Red stain (cat# S8060), and Hematoxylin and eosin (H&E) kit (cat# G1120) were obtained from Solarbio Life Sciences (Beijing, China). The CDK9 selective inhibitor NVP-2 was bought from MedChemExpress (Monmouth Junction, NJ, USA) [13, 14]. For in vitro experiments, NVP-2 was dissolved in dimethyl sulfoxide, and for in vivo studies, it was dissolved in a 1% carboxymethylcellulose sodium solution.

Animal experiments

The whole-body *Otud1*-deficient (*Otud1*$^{-/-}$) mice on a C57BL/6 genetic background were graciously supplied by professor Fuping You from Peking University Health Science Center in Beijing, China [15]. The littemate C57BL/6J wild-type (WT) mice were procured from the Animal Center of Wenzhou Medical University (WMU). Supplementary Table S1 contains the sequences of the genotyping primers. The mice were kept in a facility free of specific pathogens and given unrestricted access to food and water. The experiments were authorized by the WMU Animal Policy and Welfare Committee (Approval Document No. wydw 2021-1016). All animal experiments conformed the National Institutes of Health guidelines (Guide for the care and use of laboratory animals). The mice were subjected to a 12-h light and 12-h dark cycle while being kept at consistent room temperature. They were provided with a standard diet for rodents and were allowed to adjust to the laboratory environment for at least 2 weeks prior to the commencement of the investigation. The animal experiments were conducted and assessed by experimenters unaware of the treatment conditions. The animals were allocated to treatment groups in a randomized manner.

Ang II-induced hypertensive renal fibrosis model

In the study, 8-week-old male mice, either WT or *Otud1*$^{-/-}$, were subjected to a 4-week administration of Ang II (1 μg/kg per min) or saline solution delivered through an Alzet micro-osmotic pump (Model 1004; Cupertino, CA, USA). Animals were randomly allocated into one of four groups, with six specimens per group: WT-Sham, WT-Ang II, *Otud1*$^{-/-}$-Sham, and *Otud1*$^{-/-}$- Ang II. Throughout this period, weekly blood pressure readings were conducted with a tail-cuff, utilizing a telemetry system (BP-2010A, Softron Biotechnology).

Another segment of the experiment involved treating mice with the CDK9 inhibitor NVP-2. NVP-2 was administered by intraperitoneal injection to mice at dose levels of 5 mg·kg^{-1}·d^{-1} during the last 2 weeks of Ang II infusion. Mice for this segment were randomly assigned into four groups, again with six specimens each: WT-Sham, WT-Ang II, NVP-2-Ang II, and NVP-2-Sham. Following the completion of 4 weeks of Ang II or saline treatment, euthanasia was performed on the specimens under sodium pentobarbital anesthesia. Then, urine, blood, and kidney samples were harvested for further examination. The commercial kits sourced from Nanjing Jiancheng Bioengineering Institute, China were utilized, and the levels of Alb in urine, Cr, and BUN in serum were identified. Lastly, to quantify Ang II protein concentrations in the tissue lysates, a commercial ELISA kit was put to use.

Adeno-associated virus infection in Ang II-induced mice

It has been reported that AAV9 exhibits expression in systemic tissues, except for the testes and lungs [16]. Accordingly, WT mice were infected with either an empty vector (AAV9-NC) or AAV9 carrying the OTUD1 gene (AAV9-OTUD1). During 4 weeks, mice aged 6 weeks received injections of AAV9 via the tail vein every month (2×10^{11} particles/mouse). A 2-week saline or Ang II infusion was conducted. For this model, a total of 24 WT mice were utilized, divided into four experimental cohorts ($n = 6$ per group): AAV9-OTUD1 + Ang II, AAV9-NC + Ang II, AAV9-OTUD1, and AAV9-NC.

Ang II level measurement

The quantification of Ang II levels was carried out post-homogenization of mouse kidney tissues using a commercial ELISA kit designed for Ang II. Additionally, mouse blood samples were procured, centrifuged for serum extraction, and subsequently tested for Ang II levels using the same ELISA kit.

Immunostaining and histological analysis

Mouse kidney tissues were prepared for histological examination by undergoing a process of paraffin embedding. These paraffin-embedded specimens were sectioned (5 μm) for subsequent staining with Picro Sirius Red, Masson's Trichrome, or H&E staining. The resultant images were captured with a Nikon epifluorescence microscope (Nikon, Tokyo, Japan).

For immunofluorescence staining, these sections were exposed to a permeabilization process with 0.1% Triton X-100 for a 10-min duration and subsequently blocked using bovine serum albumin (2%) for 45 min. These samples were then allowed to incubate with primary antibodies, specifically OTUD1 (1:200), AQP-1 (1:100), and desmin (1:200), overnight at a temperature of 4 °C. The application of fluorophore-linked secondary antibodies was allowed for the detection process. Following a brief counterstaining process with 4′, 6-diamidino-2-phenylindole (DAPI) for 5 min, images were captured using the Nikon A1 laser confocal microscope.

Cell culture

Mouse kidney Transformed C3H Mouse Kidney-1 cells (TCMK-1 cells; BFN608006425) were procured from the BLUEFBIO Biotechnology

Development Co., Ltd (Shanghai, China). Mouse renal glomerular mesangial cells (SV40 MES-13 cells; #GNM21), and human embryonic kidney epithelial 293 T cells (HEK 293 T; #GNHu17) were procured from the Cell Culture Collection of the Chinese Academy of Sciences (Shanghai, China). The TCMK-1 epithelial cell lines were sustained in DMEM supplemented with 1.5 g/L sodium bicarbonate and 4.5 g/L glucose, along with 5% fetal bovine serum (FBS), 100 U/mL penicillin, and 100 mg/mL streptomycin. SV40 MES-13 cells were cultured in a 3:1 blend of DMEM and Ham's F12 medium inclusive of 14 mM HEPES, in addition to the above-mentioned supplements. The culture medium for HEK-293T cells comprised DMEM supplemented with 10% FBS, 1% penicillin/streptomycin, and 4.5 g/L glucose.

Otud1 gene silencing

Gene expression was modulated through the application of specific siRNA sequences, which facilitated the silencing of *Otud1* gene. The precise sequences of the *Otud1* siRNA and the control scrambled siRNA can be found in Supplementary Table S2. In the transfection process, 50 nM siRNA was combined with 2 μL of Lipofectamine 2000 (Thermo Fisher) in 200 μL of serum-free Opti-MEM and allowed to incubate at ambient temperature for 20 min. Following this incubation period, this mixture was introduced to TCMK-1 cells cultured in DMEM containing FBS, except antibiotics. Subsequent incubation of these cells was then performed for 24 h.

Plasmids construction and transfection

Plasmids encoding Flag-OTUD1, Flag-OTUD1 (C320S), HA-CDK9, Myc-UB, Myc-K63, and Myc-K48 were constructed by Genechem (Shanghai, China). All constructs were confirmed by DNA sequencing. Plasmids were transiently transfected into TCMK-1 cells and HEK-293T cells with Lipofectamine 3000 reagent (Invitrogen, Carlsbad, CA, USA) according to the manufacturer's instructions.

Western blotting and Co-IP analysis

Protein content from tissue samples of mice and cells cultured in vitro was procured using a RIPA buffer (P0013C; Beyotime Biotechnology, Shanghai, China). The Bradford assay by Thermo Fisher was utilized to assess protein concentration. Separation of proteins in equivalent quantities was accomplished through sodium dodecyl sulfate-polyacrylamide gel electrophoresis (SDS-PAGE). Subsequently, these proteins were transferred onto PVDF membranes, followed by a blocking step with 5% skim milk solution at room temperature lasting for an hour. Incubation with primary antibodies was carried out at 4 °C across an overnight duration. After this step, membranes were washed and further exposed to secondary antibodies conjugated with horseradish peroxidase for 1 h under ambient conditions. A chemiluminescence reagent was used to visualize immunoreactivity.

In the context of Co-IP analyses, a fraction of the lysate was retained. The rest of the lysate was left to incubate with specific antibodies at 4 °C overnight. This was followed by the introduction of magnetic beads to the lysate, which was incubated at 4 °C for 2 h. Following centrifugation, the supernatant was removed and disposed of. The complex of magnetic beads and antibodies underwent a washing process using PBS and was subsequently treated with a buffer containing SDS. The aforementioned specimens were allocated for subsequent examination via Western blotting.

Quantitative Real-time PCR analysis

RNA extraction was accomplished with TRIzol, followed by a reverse transcription of the extracted RNA into cDNA using the PrimeScript RT reagent Kit (DRR037A; Takara, Japan). The experiment involved conducting qPCR using TB Green Premix Ex Taq II (RR82WR; Takara) on the CFX96 Touch Real-Time PCR Detection System (Bio-Rad; Hercules, CA, USA). Normalization of data was carried out with reference to *Actb*. Sangon Biotech (Shanghai, China) provided the primers (Supplementary Table S1).

Statistical analysis

The data are presented as the mean ± SEM. The study utilized a one-way analysis of variance (ANOVA) with the LSD adjustment for multiple comparisons to detect differences between groups. When there was a need to obtain measurements from a single mouse multiple times, we conducted a two-way repeated-measures ANOVA analysis on each data set separately. This analysis involved using a single pooled variance and applying a Tukey correction for pairwise comparisons within groups for each data set. A significance level of $P < 0.05$ was used to determine if there was a statistically significant difference. All data analyses were conducted using SPSS 21.0.

RESULTS

OTUD1 is upregulated in kidney tissues of mice challenged with Ang II

To investigate the alteration of OTUD1 in hypertensive nephropathy, we employed subcutaneous implantation of Ang II micropumps (1 μg/kg per min) in WT mice, thereby inducing hypertension. Four weeks post-modeling, the mice were euthanized, and their kidneys were collected for examination. We examined the *Otud1* gene expression in the kidney tissues from both control and Ang II-infused mice. Figure 1a showed that OTUD1 was significantly increased in the kidney of mice challenged with Ang II. Elevation of OTUD1 in kidney tissue lysates from Ang II-treated mice was substantiated via immunoblotting (Fig. 1b, Supplementary Fig. S1a). To identify the origin of the escalated OTUD1 in the kidney, tissue samples were stained for OTUD1, AQP-1 (a tubular epithelial cell marker), and desmin (a mesangial cell marker). The immunofluorescence double-staining of kidney tissues demonstrated OTUD1 was mainly expressed in AQP-1-positive tubular epithelial cells (Fig. 1c). Subsequently, these observations were confirmed in TCMK-1 and SV40 MES-13 cells. We detected the protein levels of OTUD1 in Ang II-challenged TCMK-1 and SV40 MES-13 cells. As shown in the Fig. 1d and Supplementary Fig. S1b, the OTUD1 protein in TCMK-1 cells was significantly increased compared to the Ctrl group, while Ang II did not induce OTUD1 protein expression in SV40 MES-13 cells. The results indicate that OTUD1 in tubular epithelial cells may be involved in Ang II-induced HRD.

Otud1 deficiency alleviates Ang II-induced hypertensive renal injury

To investigate the role of OTUD1 in HRD, we constructed and utilized *Otud1*$^{-/-}$ mice (Supplementary Fig. S2a). Immunofluorescence staining using the kidney tissue of *Otud1*$^{-/-}$ mice validated the deletion of *Otud1* and also confirmed the specificity of the anti-OTUD1 antibody. WT and *Otud1*$^{-/-}$ mice were treated with either Ang II or saline at 1 μg/kg per min for 4 weeks. Mice of both genotypes that received Ang II exhibited increased systolic blood pressure, arterial pressure, and diastolic blood pressure (Fig. 2a, Supplementary Fig. S2c, d), as well as elevated Ang II plasma levels (Supplementary Fig. S2e) relative to their saline-infused counterparts. This indicates that the absence of *Otud1* does not influence blood pressure in response to Ang II. Kidney Injury Molecule-1 (KIM-1) has been proposed as a potential urinary or serological marker in renal diseases [17, 18]. In line with this, mRNA expression of the *Kim-1* gene surged significantly in kidney tissues of Ang II-infused WT mice, while *Otud1* deficiency appeared to confer protection against Ang II-triggered kidney injury (Fig. 2b).

Several vital indicators of renal function include Cr, BUN, and Alb. Compared to the WT mice, hypertensive mice exhibited higher Cr (Fig. 2c), BUN (Fig. 2d), and Alb:Cr ratio (Fig. 2e), suggesting that Ang II infusion intensifies HRD. Such responses were absent in *Otud1*$^{-/-}$ mice post-Ang II treatment. Subsequently, histopathological changes in kidney specimens were assessed. H&E staining corroborated kidney injury changes in Ang II-challenged WT mice

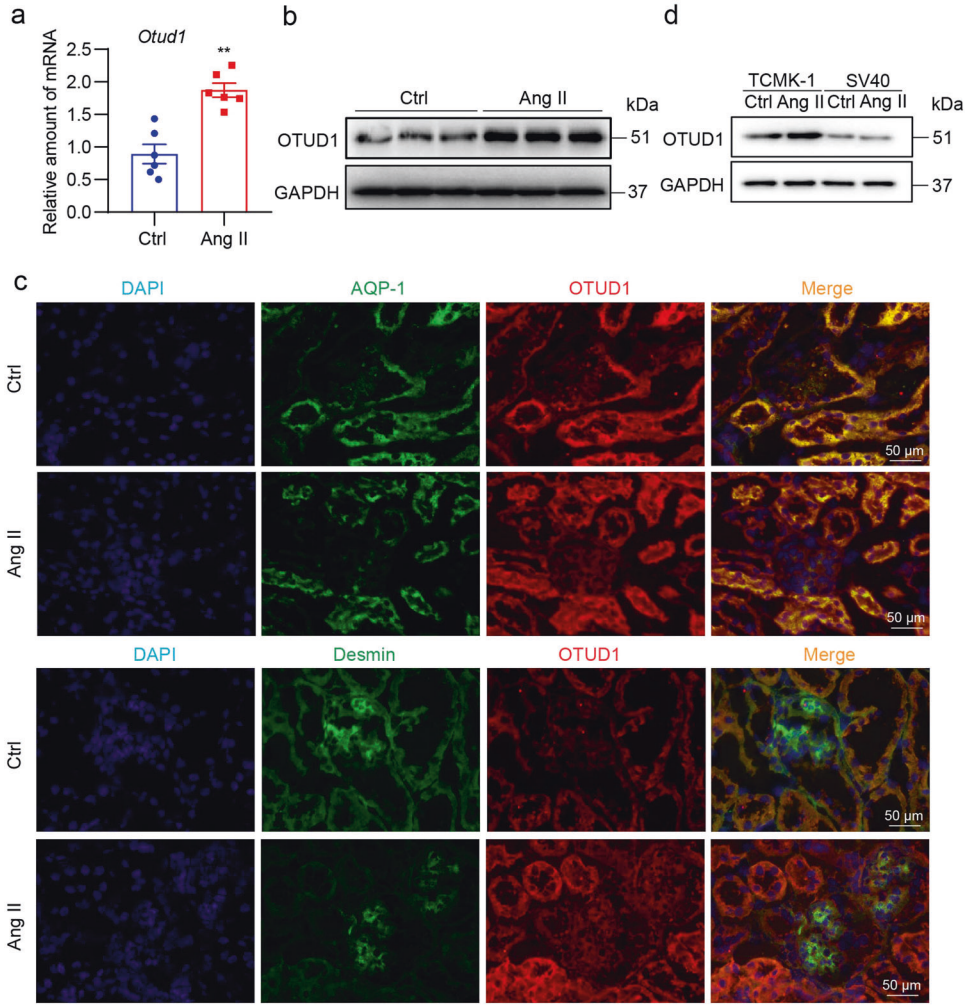

Fig. 1 OTUD1 deficiency alleviates Ang II-induced hypertensive renal injury. a mRNA levels of the *Otud1* gene in kidney tissues of mice. Data were normalized to *Actb*. **b** Representative Western blot analysis for OTUD1 levels in Ctrl and Ang II-infused kidney tissues. GAPDH was used as loading control. **c** Immunofluorescence staining of mouse kidney tissues for OTUD1 (red), AQP-1 (green), and desmin (green). Sections were counterstained with DAPI (blue). Arrows showing OTUD1-positive cells (scale bar = 50 μm). **d** Representative Western blot analysis for OTUD1 protein levels in TCMK-1 and SV40 cells. GAPDH was used as loading control. All quantitative data are presented as Mean ± SEM; $n = 6$ or $n = 3$; $^{**}P < 0.01$ vs. Control group.

(Fig. 2f, Supplementary Fig. S2f). *Otud1*$^{-/-}$ mice did not display these pathological and injury responses post-Ang II treatment. Renal fibrosis, a crucial pathological hallmark of HRD, was studied further to ascertain the role of OTUD1. Picro Sirius Red and Masson's Trichrome staining revealed diminished fibrosis in *Otud1*$^{-/-}$ mice relative to WT counterparts (Fig. 2g, h, Supplementary Fig. S2g, h). Mirroring the histological analysis, fibrosis-associated factors, COL-IV and TGF-β1, were substantially subdued in *Otud1*$^{-/-}$ mice post-Ang II infusion (Fig. 2i, j). Further, mRNA expression of fibrosis and inflammatory genes increased dramatically in kidney tissues of Ang II-infused WT mice (Fig. 2k, l), while these changes are reversed in *Otud1*$^{-/-}$ mice. Collectively, these findings illustrate that a deficiency in *Otud1* safeguards against Ang II-induced kidney injury.

Overexpression of OTUD1 aggravates Ang II-induced hypertensive renal injury

Next, we set out to investigate whether the overexpression of OTUD1 could intensify renal impairment in the Ang II-induced hypertension model. We generated AAV9 particles encoding OTUD1 and delivered them intravenously to mice via tail vein, followed by saline or Ang II infusion for 2 weeks. Successful AAV9 infection was validated by the increased expression of OTUD1 in the kidney tissues (Supplementary Fig. S3a, b). Predictably, Ang II levels rose in all mice treated with Ang II (Supplementary Fig. S3c), leading to increased systolic blood pressure, arterial pressure, and diastolic blood pressure (Fig. 3a, Supplementary Fig. S3d, e). The mRNA levels of the *Kim-1* gene were significantly amplified in kidney tissues of Ang II-infused WT mice. In line with our hypothesis, OTUD1 expression augmented Ang II-mediated kidney injury (Fig. 3b). This was further supported by the escalated levels of Cr, BUN, and Alb: Cr ratio in OTUD1-overexpressing kidney tissues (Fig. 3c–e).

Comprehensive histological assessments indicated that OTUD1 expression bolstered Ang II-induced responses, leading to kidney injury (Fig. 3f–h, Supplementary Fig. S3f–h). Following these results, fibrotic factors surged in mice exhibiting kidney OTUD1 expression in response to the Ang II challenge (Fig. 3i–k). We also discovered increased inflammatory genes in mice with kidney OTUD1 expression subjected to Ang II treatment (Fig. 3l). These findings collectively affirm that OTUD1 facilitates Ang II-induced kidney injury.

OTUD1 regulates fibrotic and inflammatory responses in TCMK-1 cells

We aimed to further elucidate the role of OTUD1 in renal cells by focusing on TCMK-1 cells. Upon exposure of TCMK-1 cells to Ang II,

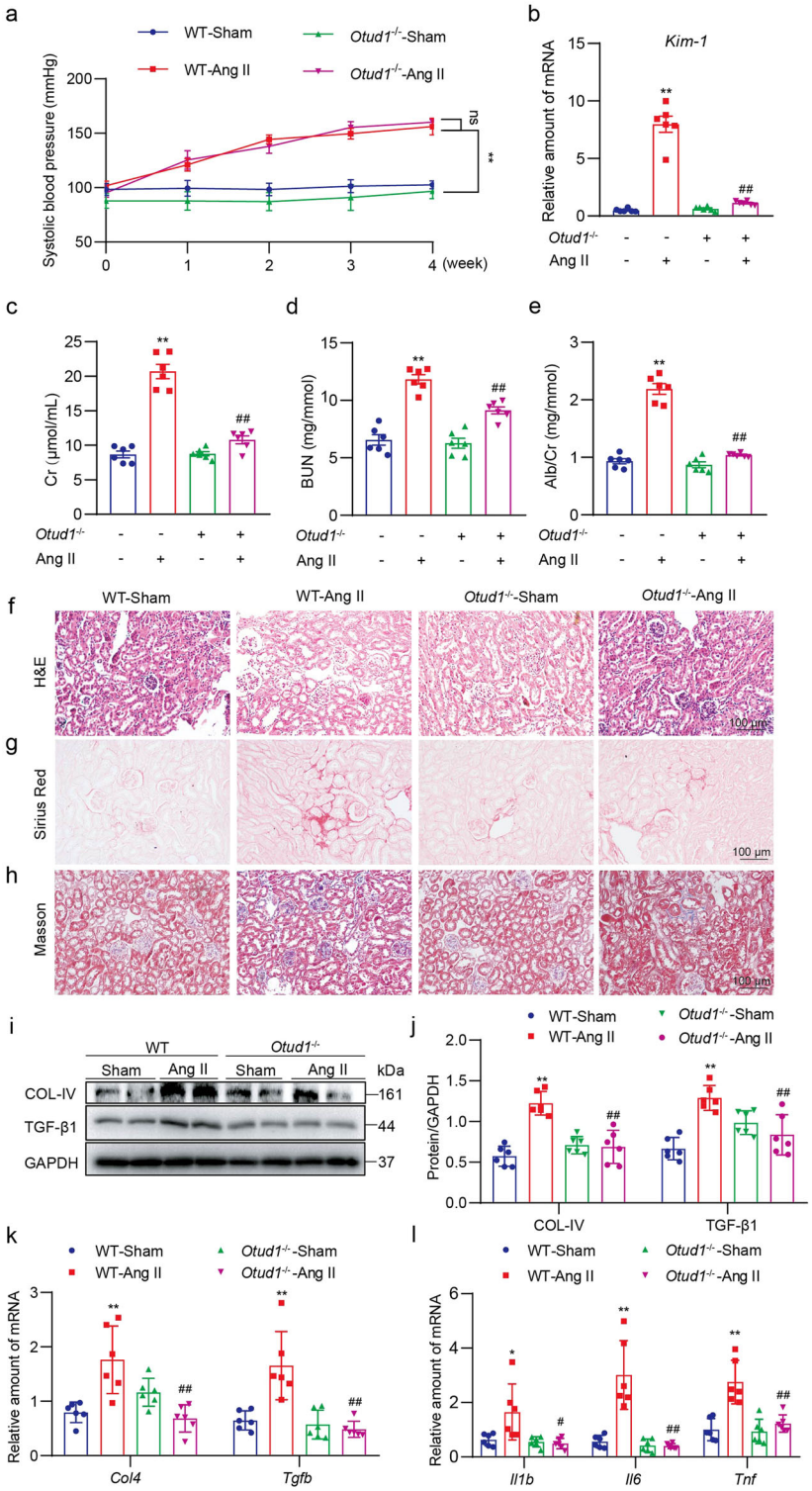

Fig. 2 ***Otud1*** **deficiency alleviates Ang II-induced hypertensive renal injury.** Wild-type and *Otud1* knockout mice were infused with saline (Sham) or Ang II for 4 weeks. **a** Systolic blood pressure was determined by non-invasive tail-cuff on a weekly basis. **b** mRNA levels of *Kim-1* in kidney tissues of mice. Data were normalized to *Actb*. **c** Serum creatinine levels in serum of mice. **d** Blood urea nitrogen levels in serum of mice. **e** Renal function was assessed in mice by measuring urine albumin to creatinine ratio at week 4. **f** H&E staining of kidney tissues (scale bar = 100 μm). **g** Fibrosis in kidney tissues was determined by Picro Sirius Red staining (scale bar = 100 μm). **h** Fibrosis in kidney tissues was determined by Masson's Trichrome staining (scale bar = 100 μm). **i, j** Western blot analysis of fibrosis-associated proteins COL-IV and TGF-β1 in kidney tissues. GAPDH was used as the loading control. Densitometric quantification is shown in (**i**). **k** mRNA levels of fibrosis-associated genes in kidney tissues of mice. Data were normalized to *Actb*. **l** mRNA levels of inflammatory genes in kidney tissues of mice. Data were normalized to *Actb*. All quantitative data are presented as Mean ± SEM; $n = 6$; $^{**}P < 0.01$ and $^{*}P < 0.05$ vs. WT-Sham group; $^{\#}P < 0.05$ and $^{\#\#}P < 0.01$ vs. WT-Ang II group.

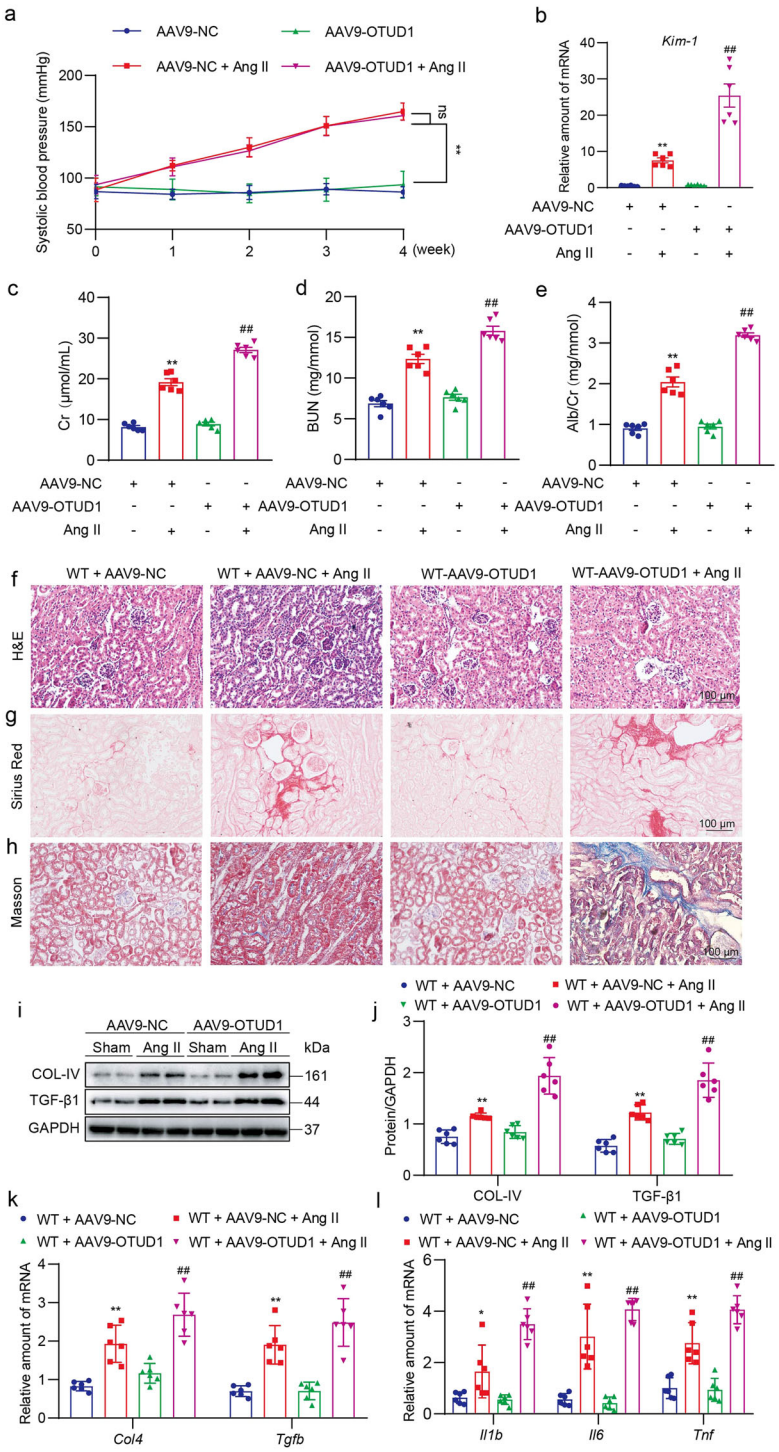

Fig. 3 Overexpression of OTUD1 aggravates Ang II-induced hypertensive renal injury. C57BL/6 mice received two injections of AAV9 encoding OTUD1, one month apart. Saline or Ang II was then infused for 2 weeks. **a** Systolic blood pressure was determined by non-invasive tail-cuff on a weekly basis. **b** mRNA levels of *Kim-1* in kidney tissues of mice. Data were normalized to *Actb*. **c** Serum creatinine levels in serum of mice. **d** Blood urea nitrogen levels in serum of mice. **e** Renal function was assessed in mice by measuring urine albumin to creatinine ratio at week 4. **f** H&E staining of kidney tissues (scale bar = 100 μm). **g** Fibrosis in kidney tissues was determined by Picro Sirius Red staining (scale bar = 100 μm). **h** Fibrosis in kidney tissues was determined by Masson's Trichrome staining (scale bar = 100 μm). **i**, **j** Western blot analysis of fibrosis-associated proteins COL-IV and TGF-β1 in kidney tissues. GAPDH was used as the loading control. Densitometric quantification is shown in (**i**). **k** mRNA levels of fibrosis-associated genes in kidney tissues of mice. Data were normalized to *Actb*. **l** mRNA levels of inflammatory genes in kidney tissues of mice. Data were normalized to *Actb*. All quantitative data are presented as Mean ± SEM; $n = 6$; $^{*}P < 0.05$, $^{**}P < 0.01$ vs. AAV9-NC group; $^{\#\#}P < 0.01$ vs. AAV9-NC + Ang II group.

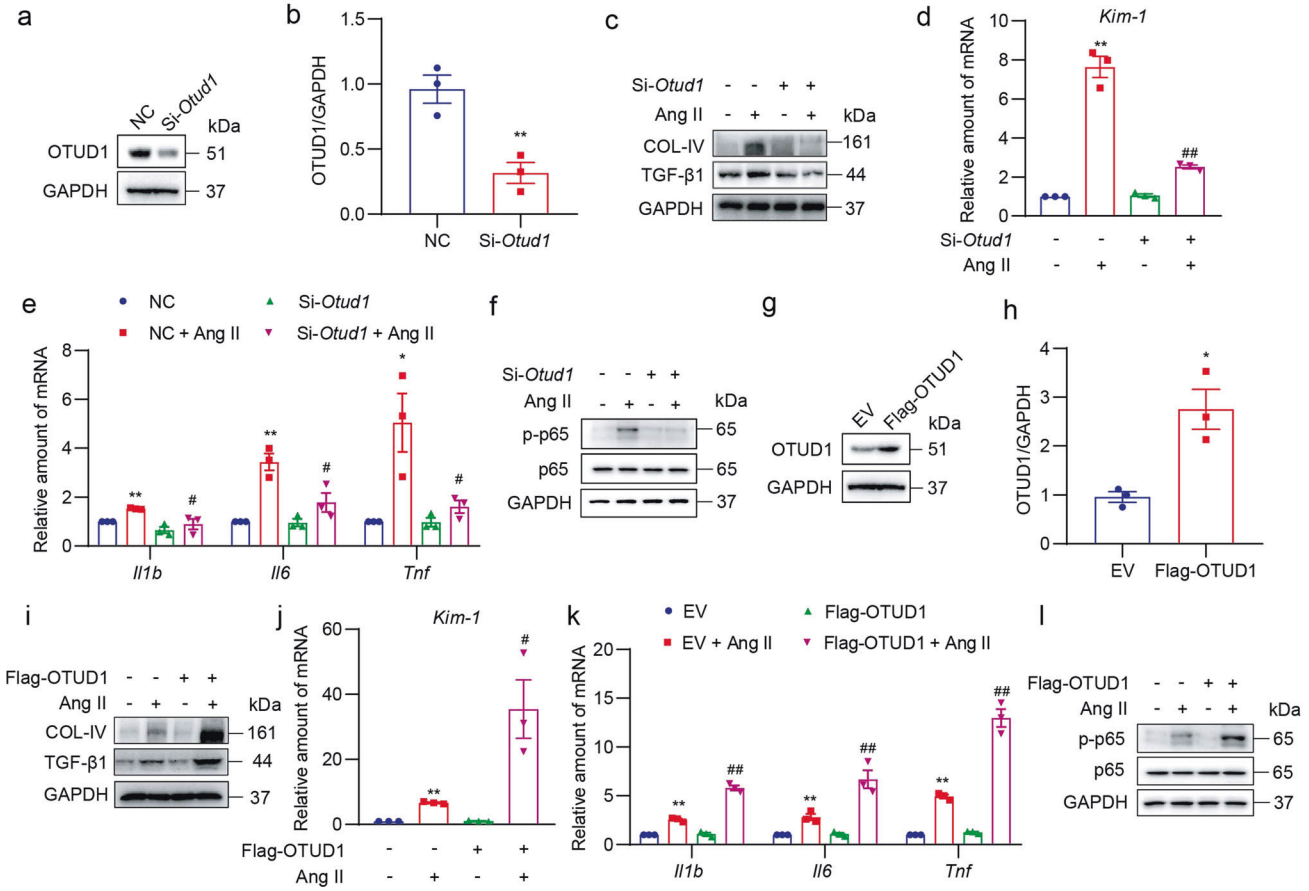

Fig. 4 OTUD1 regulates fibrotic and inflammatory responses in TCMK-1 cells. a, **b** *Otud1* gene silencing was performed in TCMK-1 by siRNA (si-*Otud1*). Negative control (NC) included scrambled siRNA transfections. After 48 h, levels of OTUD1 proteins were detected by immunoblotting (**a**) and densitometric quantification (**b**). **c** TCMK-1 cells were transfected with siRNA against *Otud1*. Cells were then exposed to 1 μM Ang II for 12 h. Western blot analysis of COL-IV and TGF-β1 proteins in TCMK-1 cells. **d** mRNA levels of *Kim-1* in TCMK-1 cells. **e** mRNA levels of inflammatory genes in TCMK-1 cells. **f** TCMK-1 cells were transfected with siRNA against *Otud1*. Levels of p65 phosphorylation were measured by immunoblotting, with total p65 and GAPDH as loading controls. **g**, **h** OTUD1 was overexpressed in TCMK-1 using Flag-tagged OTUD1 plasmid, with empty vector (EV) as control. After 48 h, levels of OTUD1 proteins were detected by immunoblotting (**g**) and densitometric quantification (**h**). **i** TCMK-1 cells were transfected with OTUD1-expressing vector. Cells were then exposed to 1 μM Ang II for 12 h. Western blot analysis of COL-IV and TGF-β1 proteins in TCMK-1 cells. **j** RNA level of *Kim-1* gene was measured. **k** mRNA levels of inflammatory genes in TCMK-1 cells. **l** TCMK-1 cells were transfected with OTUD1-expressing plasmid. Levels of p65 phosphorylation were measured by immunoblotting, with total p65 and GAPDH for normalization. All quantitative data are presented as Mean ± SEM; $n = 3$; $^{*}P < 0.05$ and $^{**}P < 0.01$ vs. Control group; $^{\#}P < 0.05$ and $^{\#\#}P < 0.01$ vs. Ang II-treated group.

OTUD1 levels swiftly escalated, with the peak activation noted at an Ang II concentration of 1 μM (Supplementary Fig. S4a, b). We then treated TCMK-1 cells with 1 μM Ang II for varying durations and assessed OTUD1 protein levels. Our findings reveal that Ang II enhances the OTUD1 levels within 60 min of exposure (Supplementary Fig. S4c, d). We silenced *Otud1* in TCMK-1 cells using siRNA (Fig. 4a, b) and then exposed the cells to Ang II at 1 μM. Western blot assay showed that Ang II stimulation increased the levels of fibrosis-associated factors, while *Otud1* knockdown reversed these changes (Fig. 4c, Supplementary Fig. S4e, f). Moreover, our observations indicated that *Otud1* knockdown prevented the increase in *Kim-1* gene in Ang II-infused TCMK-1 cells (Fig. 4d). Consistent with our findings on mouse model, Ang II challenge failed to induce inflammatory gene overexpression in TCMK-1 cells when Otud1 was silenced (Fig. 4e). Furthermore, the knockdown of *Otud1* in TCMK-1 cells impeded Ang II-induced increase of phosphorylated p65 level (Fig. 4f and Supplementary Fig. S4g).

In a subsequent step, we introduced OTUD1 expression into TCMK-1 cells (Fig. 4g, h) and repeated similar experiments. Our data demonstrate that OTUD1 expression amplifies the fibrotic, injury, and inflammatory responses of TCMK-1 cells to Ang II (Fig. 4i–k; Supplementary Fig. S4h, i). Overexpression of OTUD1 in TCMK-1 cells also resulted in an augmentation of Ang II-induced p65 phosphorylation (Fig. 4l and Supplementary Fig. S4j). These results substantiate that OTUD1 is necessary for Ang II to induce inflammation and fibrotic factor expression in TCMK-1 cells.

OTUD1 mediates Ang II-mediated CDK9 activation in both kidney tissues and TCMK-1 cells

Deubiquitinating enzymes modulate biological processes by modulating the degradation or activity of substrate proteins. Recent studies have indicated that CDK9 may play a potential role in inflammatory responses and renal fibrosis [19]. Thus, we may hypothesize the regulation of OTUD1 on CDK9. We conducted a co-IP assay after transfecting TCMK-1 cells and 293 T cells with Flag-tagged OTUD1. Our results, shown in Fig. 5a and Supplementary Fig. S5a, indicate that CDK9 does indeed interact with OTUD1. In a prior investigation, elevated p-(Thr186) CDK9 levels, as the activated form of CDK9, contributed to the renal inflammation and fibrosis [20]. In this study, we evaluated the levels of Thr186 p-CDK9 after modulating OTUD1 in TCMK-1 cells. We first inhibited the expression of *Otud1* in TCMK-1 cells and subsequently subjected these cells to a 12-h exposure of 1 μM

Ang II. In this particular scenario, the inhibition of *Otud1* impeded the increase of phosphorylated CDK9 levels induced by Ang II in TCMK-1 cells (Fig. 5b and Supplementary Fig. S5b). On the other hand, the induction of OTUD1 expression in TCMK-1 cells resulted in an augmentation of Ang II-triggered p-CDK9 (Fig. 5c and Supplementary Fig. S5c). Figure 5b, c demonstrates that the expression level of CDK9 remained unaltered in cells upon the influence of OTUD1. Based on the observations, it can be inferred that OTUD1 interacts with CDK9 and regulates CDK9 activity.

We determined whether OTUD1 deficiency and overexpression modified CDK9 in the kidney of Ang II-infused mice. An analysis of kidney tissue lysates revealed that Ang II enhanced CDK9 phosphorylation in WT mice, but these activity measures were diminished in *Otud1*$^{-/-}$ mice (Fig. 5d and Supplementary Fig. S5d). Conversely, OTUD1 expression amplified Ang II-mediated p-CDK9 (Fig. 5e and Supplementary Fig. S5e). Together, these in vitro and in vivo studies demonstrate that OTUD1 interacts with CDK9 and regulates Thr186 phosphorylation to modulate the expression of inflammatory and fibrosis-associated genes. In our experimental conditions, a selective CDK9 inhibitor, NVP-2, lowered the protein and mRNA levels of inflammatory and fibrosis-associated genes in TCMK-1 cells exposed to Ang II, even when OTUD1 was expressed (Fig. 5f–h, Supplementary Fig. S5f). In addition, we found that Ang II/OTUD1-induced p65 phosphorylation was significantly reversed by CDK9 inhibition, indicating that CDK9 mediates Ang II/OTUD1-regulated NF-κB activity (Fig. 5i, j).

OTUD1 regulates the activity of CDK9 through deubiquitination

Further investigation was conducted on the mechanism through which OTUD1 modulates the activity of CDK9. In HEK-293T cells co-transfected with plasmids encoding CDK9 (HA-tagged) and OTUD1 (Flag-tagged) proteins, we showed that OTUD1 removed the ubiquitin chains from CDK9 (Fig. 6a). Generally, K48-linked ubiquitination regulates the degradation and stability of the substrate proteins, while K63-linked ubiquitination generally regulates the structure and function of the substrates [21, 22]. Here, we found that OTUD1 did not alter the total protein level of CDK9 but increased CDK9 phosphorylation, indicating that OTUD1 deubiquitinates CDK9 likely through a K63-dependent manner. As expected, data in Fig. 6b showed that OTUD1 could deubiquitinated CDK9 through the K63 ubiquitin chain. OTUD1 failed to remove the K48-linked ubiquitin from CDK9 (Supplementary Fig. S6). This result confirmed that OTUD1 deubiquitinates CDK9 through a K63-dependent manner. Subsequently, we induced mutations in the active sites of OTUD1 by substituting cysteine with serine at position 320. Our findings indicate that the OTUD1C320S mutant was incapable of eliminating UBs from CDK9, as illustrated in Fig. 6c. The aforementioned observations offer empirical support for the proposition that the cysteine residue situated at position 320 within OTUD1 plays a role in the elimination of UB molecules from CDK9, thus impeding its degradation.

OTUD1 alleviates Ang II-induced hypertensive renal injury by regulating CDK9

Mice were infused with either saline or Ang II for 4 weeks. A subgroup of the experimental mice was also treated with the CDK9 inhibitor, NVP-2, administered at 5 mg per kg daily for the final 2 weeks. Kidney structural changes induced by Ang II were examined using H&E staining. As expected, these histological alterations were markedly ameliorated in the kidneys of mice treated with NVP-2 (Fig. 7a, Supplementary Fig. S7a). Further histological evaluations of the kidneys were conducted for all mice. Picro Sirius Red and Masson's Trichrome staining confirmed that NVP-2 inhibited Ang II-induced kidney fibrosis (Fig. 7b, c, Supplementary Fig. S7b, c). Increases in protein and mRNA levels of COL-IV and TGF-β1 induced by Ang II were reversed with NVP-2 treatment, further corroborating the anti-fibrotic action of NVP-2 (Fig. 7d–f). The mRNA expression levels of inflammatory genes, including *Tnf, Il6*, and *Il1b*, were significantly elevated in the kidneys of mice infused with Ang II, and these increases were nearly completely negated by NVP-2 treatment (Fig. 7g).

DISCUSSION

This investigation aimed to examine the involvement of DUBs in the pathogenesis of renal disease associated with hypertension. These findings indicate an upregulation of OTUD1 in renal epithelial cells after the introduction of Ang II. Following exposure to the Ang II regimen, mice with a deficiency in OTUD1 exhibited a reduction in both kidney fibrosis, inflammation, and injury. Mechanistically, OTUD1 interacts with CDK9 and facilitates its deubiquitination. Additionally, it has been determined that the cysteine residue located at position 320 of the OTUD1 protein is essential in facilitating the phosphorylation of CDK9 through K63-linked deubiquitination. The principal discoveries are succinctly presented in the Graphical Abstract.

Notably, the majority of DUBs are cysteine proteases [23], with nearly 100 potential DUBs identified in humans. Research on DUBs in maladaptive kidney injury, however, remains scarce. Recently, a small number of DUBs have been recognized in various kidney fibrosis and injury models. For instance, OTUB1 was found to potentially regulate glomerulonephritides by facilitating the degradation of decorin, thereby amplifying a harmful cycle marked by increased TGF-β1 production and matrix deposition, leading to glomerulosclerosis [24]. Conversely, some DUBs have been reported to have protective effects against kidney diseases. In previous research, Park and colleagues discovered that YOD1, a member of the ovarian tumor (OTU) family of DUBs, is weakly expressed in a mouse model of unilateral ureteric obstruction [21]. They further demonstrated that YOD1 regulates the Hippo signaling pathway via NEDD4 and that NEDD4's K63-linked polyubiquitin chain has a significant role in kidney diseases [25]. Similarly, USP25 has been implicated in HRD. In an Ang II-induced HRD model, USP25 knockout mice exhibited a significant worsening of renal dysfunction and fibrosis. USP25 was found to inhibit the TGF-β pathway by reducing SMAD4's K63-linked polyubiquitination [26]. The combined effects of these DUBs could be critical to the induction of deleterious kidney fibrosis, injury, and inflammatory factors, which presents an intriguing area for future research. Interestingly, we found that OTUD1 was significantly increased in the kidneys of mice challenged with Ang II, indicating a role of OTUD1 in HRD. So far, there is only one publication involving the role of OTUD1 in kidney disease, where OTUD1 has been identified as a key gene associated with overall survival in renal clear cell carcinoma patients [27]. Therefore, our study increased new insight on DUBs mediating kidney diseases.

Studies have shown that while DUBs have been linked to a wide variety of overlapping substrates, they also exhibit specificity towards certain substrates. OTUD1 has been demonstrated to act as a DUB for peroxiredoxin 4 (PRDX4), thereby safeguarding it from undergoing endoplasmic reticulum (ER)-associated degradation. The regulatory pathway involving OTUD1-PRDX4 has not been fully described yet, but it has been found to play a significant role in driving immunoglobulin production and sensitivity to proteasome inhibitors in cells affected by multiple myeloma. This underscores the significance of OTUD1 in the proliferation of myeloma cells [28]. Recently, we have identified STAT3 and SMAD3 as substrate proteins of OTUD1 in cardiomyocytes and vascular endothelial cells, respectively [11, 12].

CDK9 has been identified as a substrate of OTUD1 in the renal system. The involvement of CDK9 in renal dysfunction has been previously documented. CDK9 has been implicated in a mouse model of unilateral ureteral obstruction that results in significant renal fibrosis, according to recent research [19]. The CDK9 protein was found to have a direct association with the expansion of the

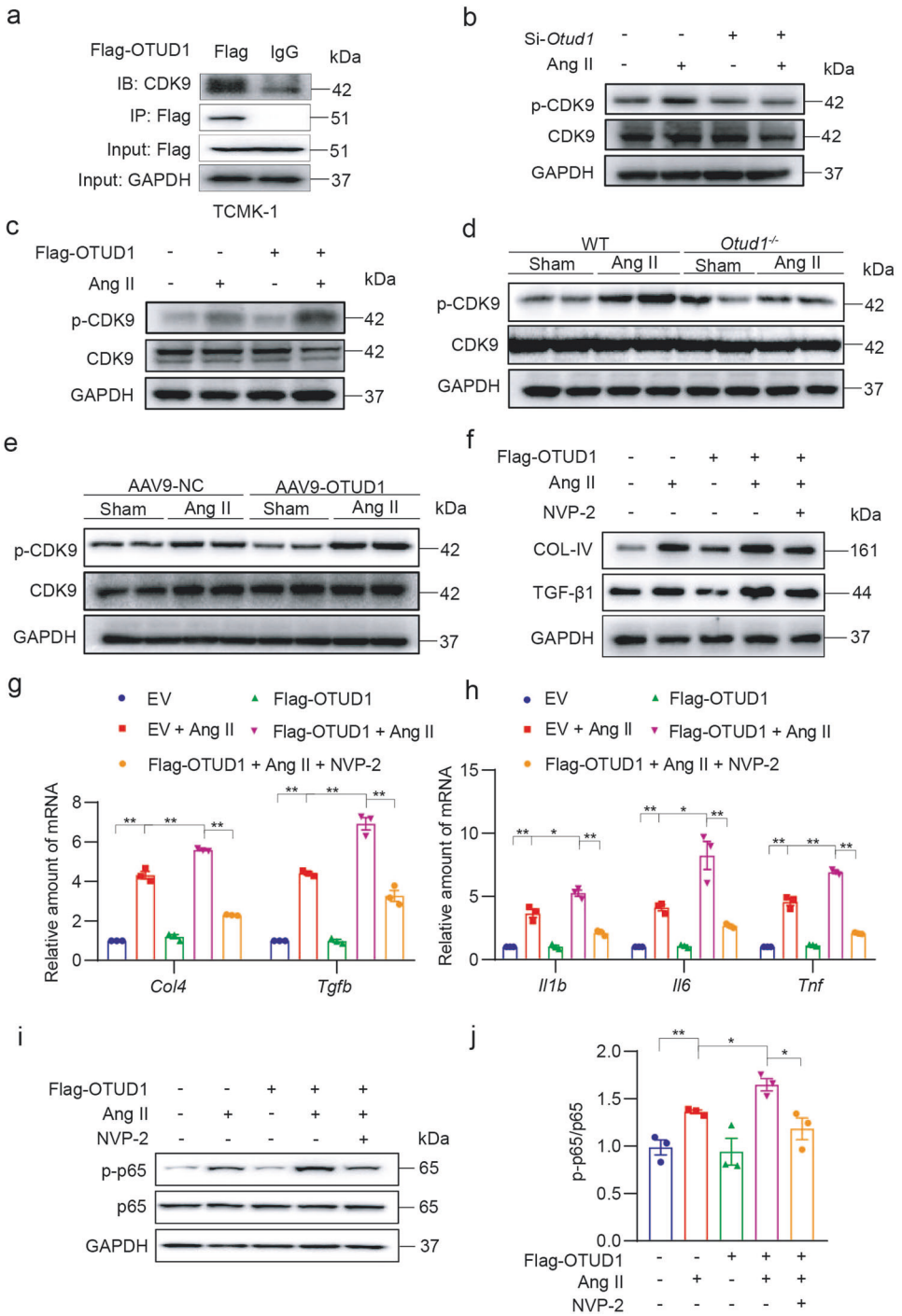

Fig. 5 OTUD1 mediates Ang II-induced CDK9 activation. a TCMK-1 cells were transfected with Flag-tagged OTUD1. Lysates from cells were immunoprecipitated with anti-OTUD1. CDK9 levels were detected by immunoblotting. IgG was used as control for IP. **b** TCMK-1 cells were transfected with siRNA against *Otud1*. Levels of CDK9 phosphorylation were measured by immunoblotting. Total CDK9 and GAPDH were used for normalization. **c** TCMK-1 cells were transfected with OTUD1-expressing vector. Levels of CDK9 phosphorylation were measured by immunoblotting. Total CDK9 and GAPDH were used for normalization. **d** Levels of p-CDK9 and CDK9 in whole kidney lysate of mice infused with Ang II for 4 weeks were detected by immunoblotting. **e** Levels of p-CDK9 and CDK9 in whole kidney lysates from mice. **f** TCMK-1 cells were transfected with OTUD1-expressing vector (Flag-OTUD1) or empty vector (EV). Cells were then challenged with 1 μM Ang II for 12 h. Some cells were treated with CDK9 inhibitor NVP-2. Western blot analysis of COL-IV and TGF-β1 proteins in TCMK-1 cells. RNA levels of fibrosis-associated genes (**g**) and inflammatory genes (**h**) were measured. Data were normalized to *Actb*. **i**, **j** TCMK-1 cells were transfected with OTUD1-expressing plasmid and then treated with CDK9 inhibitor NVP-2. Levels of p65 phosphorylation were measured by immunoblotting (**i**) and shown in densitometric quantification (**j**). Total p65 and GAPDH were used for normalization. All quantitative data are presented as Mean ± SEM; $n = 3$ or $n = 6$; $^{*}P < 0.05$ and $^{**}P < 0.01$.

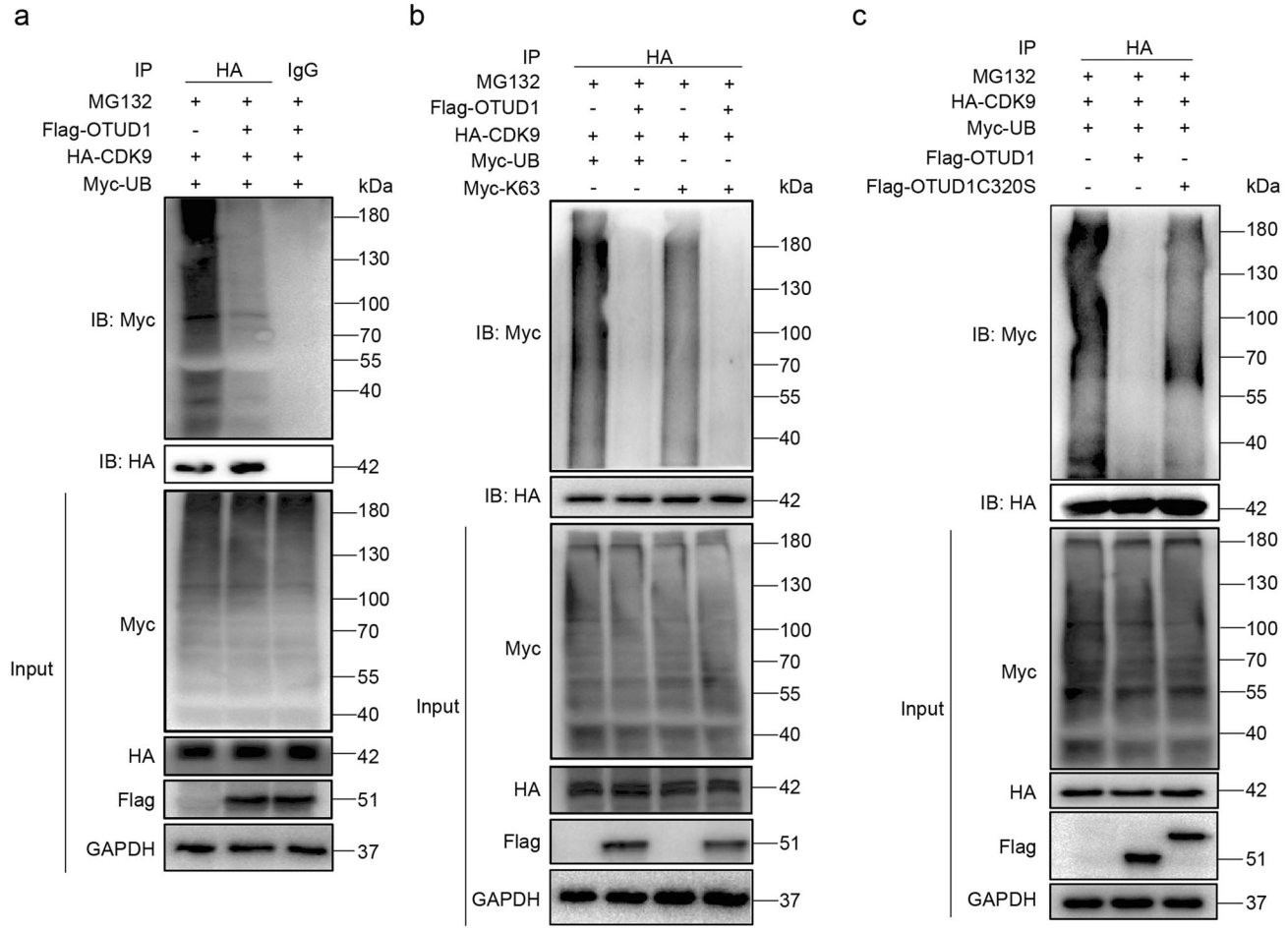

Fig. 6 OTUD1 regulates the activity of CDK9 through deubiquitination. a HEK-293T cells were transfected with HA-CDK9, Myc-UB and Flag-OTUD1. Cells were then exposed to MG132. Ubiquitinated CDK9 was detected by immunoblotting using an HA-specific antibody (control = IgG). **b** HEK-293T cells were transfected with HA-CDK9, Myc-UB, Myc-K63 and Flag-OTUD1. Cells were then exposed to MG132. Ubiquitinated CDK9 was detected by immunoblotting. **c** Immunoprecipitation of HA-CDK9 in HEK-293T cells that co-expressed Myc-UB, Flag-OTUD1 and Flag-OTUD1C320S. Ubiquitinated CDK9 was detected by immunoblotting.

extracellular matrix induced by TGF-β1 through the formation of CDK9/Smad complexes. Additionally, it has been demonstrated that the inhibition of CDK9 by flavopiridol can impede the loss of podocyte synaptophysin and mitochondrial dysfunction induced by palmitic acid, mainly by inhibiting Smad [19]. It has been reported that CDK9 is activated in the condition of diabetic nephropathy [20]. The precise mechanisms underlying CDK9 activation in HRD remain incompletely elucidated. However, our present investigation proposes a plausible mechanism wherein decreased ubiquitination and heightened protein stability, facilitated by OTUD1, may be involved.

CDK9 belongs to the serine/threonine kinase subfamily [29] and has diverse functions in cellular processes such as cell division, apoptosis, transcription, and differentiation. It has been reported that CDK9 phosphorylation at Thr186 residue in the telomere-loop (T-loop) domain is critical for the kinase activity of CDK9/P-TEFb [30], which changes the conformation of the T-loop and allows substrate and ATP into the CDK9 catalytic site [31]. A *cis*-conformation of CDK9 T-Loop has been shown to induce its autophosphorylation at Thr186 [32]. Acetylating modification of CDK9 at Lys-164 could promote T-loop autophosphorylation at Thr186 and thus CDK9/P-TEFb kinase activity, probably via inducing a *cis*-conformation of the T-loop [33, 34]. Unfortunately, no previous studies reported the effect of CDK9 ubiquitination on its phosphorylation. Our present investigation indicated that OTUD1 acts as a new DUB for CDK9 through K63-linked manner, thereby facilitating CDK9 phosphorylation. This study is the first time to report the regulation mechanism for CDK9 activity through K63-linked deubiquitination by OTUD1. It is very interesting to explore the mechanism by which CDK9 ubiquitination affects CDK9 phosphorylation. We guess that the CDK9 ubiquitination hinders the conformational transition, while OTUD1-mediated CDK9 deubiquitination induces the formation of *cis*-conformation of CDK9 T-loop, promoting CDK9 autophosphorylation at Thr186. This hypothesis deserves further investigation through structural biology methods in the future.

Inflammatory responses are widely recognized to be regulated by the NF-κB pathway as well as interferon regulatory factor pathways. Previous studies reported the regulation of OTUD1 on NF-κB activity. For example, one recent study suggested that OTUD1 could regulate NF-κB signaling [35]. Another study also indicated that OTUD1 can regulate inflammatory responses through modulating NF-κB signaling [36]. OTUD1 downregulates the NF-κB activation independently of the cleavage of linear ubiquitin chain and principally by hydrolyzing the K63-linked ubiquitin chain [35]. Another study also indicated that OTUD1 moderated intestinal inflammation by inhibiting RIPK1-mediated NF-κB activation [36]. Here, we found that Ang II/OTUD1-induced p65 phosphorylation was significantly reversed by CDK9 inhibition, indicating that CDK9 mediates Ang II/OTUD1-regulated NF-κB activity, inflammation, and subsequent renal injuries. Our study provides CDK9 as a new link between OTUD1 and NF-κB.

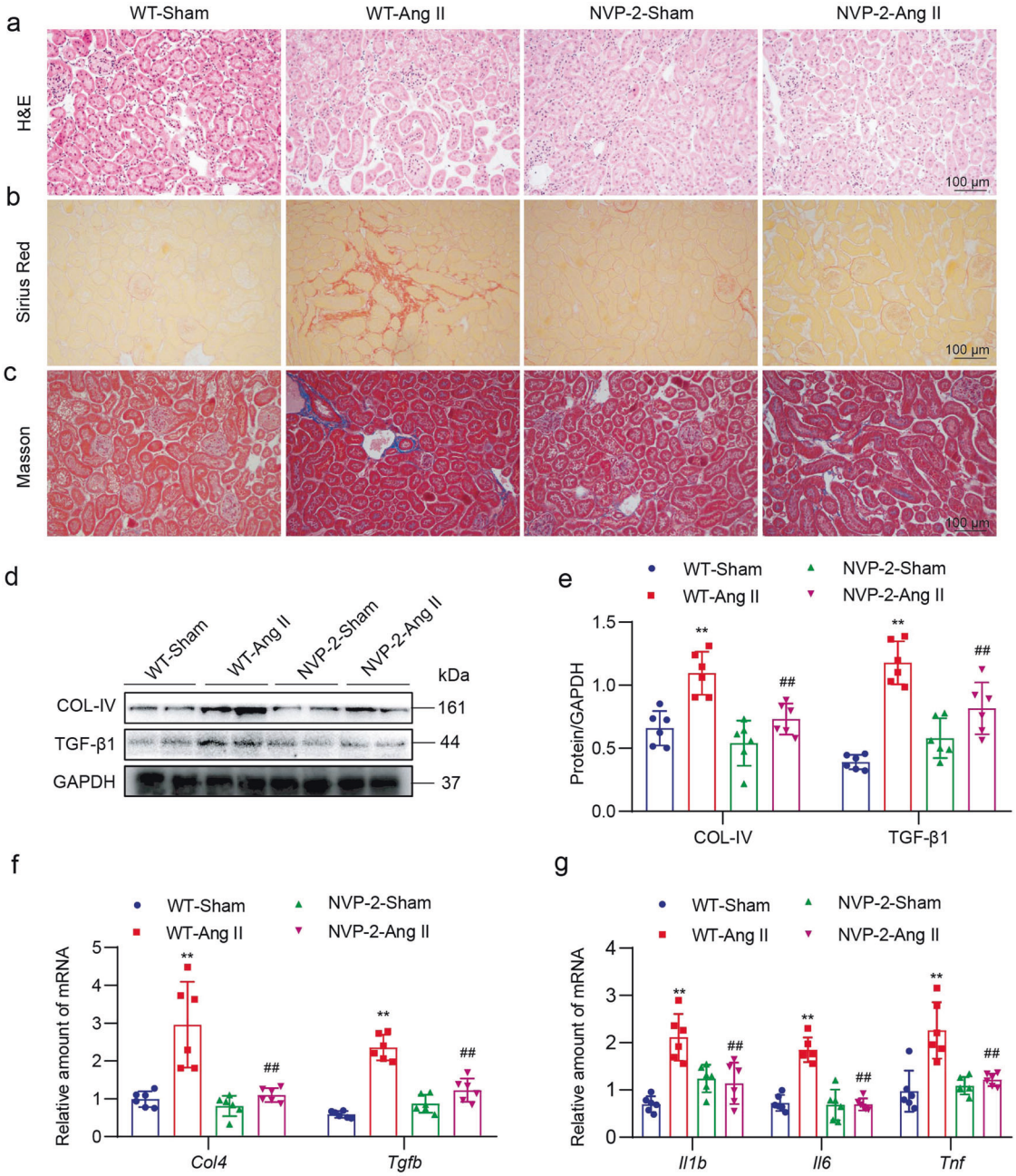

Fig. 7 OTUD1 alleviates Ang II-induced hypertensive renal injury by regulating CDK9. C57BL/6 mice were infused with saline (Sham) or Ang II for 4 weeks. Two weeks after initiating Ang II infusion, mice were treated with NVP-2. **a** H&E staining of kidney tissues (scale bar = 100 μm). **b** Fibrosis in kidney tissues was determined by Picro Sirius Red staining (scale bar = 100 μm). **c** Fibrosis in kidney tissues was determined by Masson's Trichrome staining (scale bar = 100 μm). **d** Western blot analysis of fibrosis-associated proteins COL-IV and TGF-β1 in kidney tissues. GAPDH was used as the loading control. **e** Densitometric quantification for blots in (**d**). **f** mRNA levels of fibrosis-associated genes in kidney tissues of mice. Data were normalized to *Actb*. **g** mRNA levels of inflammatory genes in kidney tissues of mice. Data were normalized to *Actb*. All quantitative data are presented as Mean ± SEM; $n = 6$ or $n = 3$; $^{**}P < 0.01$ vs. Control group; $^{\#\#}P < 0.01$ vs. Ang II-treated group.

In conclusion, our findings indicate that the inhibition of OTUD1 effectively impedes the development of kidney fibrosis, inflammation, and injury deficits induced by Ang II. On the contrary, elevated expression of OTUD1 amplifies the adverse effects of Ang II-induced renal impairments. During our mechanistic studies, we identified CDK9 as a new substrate of OTUD1 in tubular epithelial cells. OTUD1 enhances CDK9 activity through the elimination of the K63 ubiquitin chain from CDK9, leading to an upsurge in its activity to promote renal inflammation and fibrosis. Our study discovers the significance of OTUD1 in HRD, as it directly regulates the activity of CDK9 and highlights the new OTUD1-CDK9 axis as the potential targets for the treatment of HRD.

ACKNOWLEDGEMENTS

This study was supported by the National Natural Science Foundation of China (82000793 to WL and 82370829 for HZ) and the Key Discipline of Zhejiang Province in Public Health and Preventive Medicine (First Class, Category A) at Hangzhou Medical College.

AUTHOR CONTRIBUTIONS

GL, HZ, and WL contributed to the literature search and study design. MYW, TXY, QYW, XH, SJY, and XH carried out the experiments. WL and MYW contributed to data collection and analysis. MYW and WL participated in the drafting of the article. GL, YW, and XHL revised the manuscript.

ADDITIONAL INFORMATION

Supplementary information The online version contains supplementary material available at https://doi.org/10.1038/s41401-023-01192-6.

Competing interests: The authors declare no competing interests.

REFERENCES

1. Hill NR, Fatoba ST, Oke JL, Hirst JA, O'Callaghan A, Lasserson DS, et al. Global prevalence of chronic kidney disease—a systematic review and meta-analysis. PLoS One. 2016;11:e0158765.
2. Rai A, Narisawa M, Li P, Piao LM, Li YL, Yang G, et al. Adaptive immune disorders in hypertension and heart failure: focusing on T-cell subset activation and clinical implications. J Hypertens. 2020;38:1878–89.
3. Zhang J, Cao L, Wang XH, Li Q, Zhang M, Cheng C, et al. The E3 ubiquitin ligase TRIM31 plays a critical role in hypertensive nephropathy by promoting proteasomal degradation of MAP3K7 in the TGF-β1 signaling pathway. Cell Death Differ. 2022;29:556–67.
4. Zhou LL, Li YJ, Hao S, Zhou D, Tan RJ, Nie J, et al. Multiple genes of the renin-angiotensin system are novel targets of Wnt/β-catenin signaling. J Am Soc Nephrol 2015;26:107–20.
5. Lecker SH, Goldberg AL, Mitch WE. Protein degradation by the ubiquitin-proteasome pathway in normal and disease states. J Am Soc Nephrol. 2006;17:1807–19.
6. Ihara Y, Morishima-Kawashima M, Nixon R. The ubiquitin-proteasome system and the autophagic-lysosomal system in Alzheimer's disease. Cold Spring Harb Perspect Med. 2012;2:8.
7. Roberts JZ, Crawford N, Longley DB. The role of ubiquitination in apoptosis and necroptosis. Cell Death Differ. 2022;29:272–84.
8. Cockram PE, Kist M, Prakash S, Chen SH, Wertz IE, Vucic D. Ubiquitination in the regulation of inflammatory cell death and cancer. Cell Death Differ. 2021;28:591–605.
9. Oikawa D, Shimizu K, Tokunaga F. Pleiotropic roles of a KEAP1-associated deubiquitinase, OTUD1. Antioxidants. 2023;12:2.
10. Song J, Liu TT, Yin Y, Zhao W, Lin ZQ, Yin YX, et al. The deubiquitinase OTUD1 enhances iron transport and potentiates host antitumor immunity. EMBO Rep. 2021;22:e51162.
11. Wang MY, Han X, Yu TX, Wang MX, Luo W, Zou CP, et al. OTUD1 promotes pathological cardiac remodeling and heart failure by targeting STAT3 in cardiomyocytes. Theranostics. 2023;13:2263–80.
12. Huang ZQ, Shen SR, Wang MY, Li WX, Wu GJ, Huang WJ, et al. Mouse endothelial OTUD1 promotes angiotensin II-induced vascular remodeling by deubiquitinating SMAD3. EMBO Rep. 2023;24:e56135.
13. Guhan SM, Shaughnessy M, Rajadurai A, Taylor M, Kumar R, Ji ZY, et al. The molecular context of vulnerability for CDK9 suppression in triple wild-type melanoma. J Invest Dermatol. 2021;141:2018–27.
14. Olson CM, Jiang BS, Erb MA, Liang YK, Doctor ZM, Zhang ZN, et al. Pharmacological perturbation of CDK9 using selective CDK9 inhibition or degradation. Nat Chem Biol. 2018;14:163–70.
15. Zhang ZM, Wang DD, Wang PY, Zhao YC, You FP. OTUD1 negatively regulates type I IFN induction by disrupting noncanonical ubiquitination of IRF3. J Immunol. 2020;204:1904–18.
16. Zincarelli C, Soltys S, Rengo G, Rabinowitz JE. Analysis of AAV serotypes 1–9 mediated gene expression and tropism in mice after systemic injection. Mol Ther. 2008;16:1073–80.
17. Restrepo JM, Torres-Canchala L, Bonventre JV, Arias JC, Ferguson M, Villegas A, et al. Urinary KIM-1 is not correlated with gestational age among 5-year-old children born prematurely. Front Pediatr. 2023;11:1038206.
18. Karmakova TA, Sergeeva NS, Kanukoev KY, Alekseev BY, Kaprin AD. Kidney injury molecule 1 (KIM-1): a multifunctional glycoprotein and biological marker (Review). Sovrem Tekhnologii Med. 2021;13:64–78.
19. Qu XL, Jiang MJ, Sun YB, Jiang XY, Fu P, Ren Y, et al. The Smad3/Smad4/CDK9 complex promotes renal fibrosis in mice with unilateral ureteral obstruction. Kidney Int. 2015;88:1323–35.
20. Yang XJ, Luo W, Li L, Hu X, Xu MJ, Wang Y, et al. CDK9 inhibition improves diabetic nephropathy by reducing inflammation in the kidneys. Toxicol Appl Pharmacol 2021;416:115465.
21. Thrower JS, Hoffman L, Rechsteiner M, Pickart CM. Recognition of the polyubiquitin proteolytic signal. EMBO J. 2000;19:94–102.
22. Mukhopadhyay D, Riezman H. Proteasome-independent functions of ubiquitin in endocytosis and signaling. Science. 2007;315:201–5.
23. Nijman SM, Luna-Vargas MP, Velds A, Brummelkamp TR, Dirac AM, Sixma TK, et al. A genomic and functional inventory of deubiquitinating enzymes. Cell. 2005;123:773–86.
24. Zhang Y, Hu RM, Wu HJ, Jiang WN, Sun Y, Wang Y, et al. OTUB1 overexpression in mesangial cells is a novel regulator in the pathogenesis of glomerulonephritis through the decrease of DCN level. PLoS One. 2012;7:e29654.
25. Park JH, Kim SY, Cho HJ, Lee SY, Baek KH. YOD1 Deubiquitinates NEDD4 involved in the Hippo signaling pathway. Cell Physiol Biochem. 2020;54:1–14.
26. Zhao Y, Chen X, Lin YM, Li ZD, Su X, Fan SJ, et al. USP25 inhibits renal fibrosis by regulating TGFβ-SMAD signaling pathway in Ang II-induced hypertensive mice. Biochim Biophys Acta Mol Basis Dis. 2023;1869:166713.
27. Liu WT, Yan B, Yu HX, Ren JN, Peng M, Zhu L, et al. OTUD1 stabilizes PTEN to inhibit the PI3K/AKT and TNF-alpha/NF-kappaB signaling pathways and sensitize ccRCC to TKIs. Int J Biol Sci. 2022;18:1401–14.
28. Vdovin A, Jelinek T, Zihala D, Sevcikova T, Durech M, Sahinbegovic H, et al. The deubiquitinase OTUD1 regulates immunoglobulin production and proteasome inhibitor sensitivity in multiple myeloma. Nat Commun. 2022;13:6820.
29. Huang Z, Wang TQ, Wang C, Fan Y. CDK9 inhibitors in cancer research. RSC Med Chem. 2022;13:688–710.
30. Kudin AP, Bimpong-Buta NY, Vielhaber S, Elger CE, Kunz WS. Characterization of superoxide-producing sites in isolated brain mitochondria. J Biol Chem. 2004;279:4127–35.
31. Russo AA, Jeffrey PD, Pavletich NP. Structural basis of cyclin-dependent kinase activation by phosphorylation. Nat Struct Biol. 1996;3:696–700.
32. Ramakrishnan R, Dow EC, Rice AP. Characterization of Cdk9 T-loop phosphorylation in resting and activated $CD4^+$ T lymphocytes. J Leukoc Biol. 2009;86:1345–50.
33. Fu JJ, Yoon HG, Qin J, Wong JM. Regulation of P-TEFb elongation complex activity by CDK9 acetylation. Mol Cell Biol. 2007;27:4641–51.
34. Mbonye U, Wang BL, Gokulrangan G, Shi WX, Yang SC, Karn J. Cyclin-dependent kinase 7 (CDK7)-mediated phosphorylation of the CDK9 activation loop promotes P-TEFb assembly with Tat and proviral HIV reactivation. J Biol Chem. 2018;293:10009–25.
35. Oikawa D, Gi M, Kosako H, Shimizu K, Takahashi H, Shiota M, et al. OTUD1 deubiquitinase regulates NF-κB- and KEAP1-mediated inflammatory responses and reactive oxygen species-associated cell death pathways. Cell Death Dis. 2022;13:694.
36. Wu B, Qiang LH, Zhang Y, Fu YS, Zhao MY, Lei ZH, et al. The deubiquitinase OTUD1 inhibits colonic inflammation by suppressing RIPK1-mediated NF-κB signaling. Cell Mol Immunol. 2022;19:276–89.